

UC Santa Cruz

UC Santa Cruz Electronic Theses and Dissertations

Title

Smoothing the Effects of Renewable Generation on the Distribution Grid

Permalink

<https://escholarship.org/uc/item/3nr053m8>

Author

Naud, Paul S.

Publication Date

2014

Peer reviewed|Thesis/dissertation

UNIVERSITY OF CALIFORNIA
SANTA CRUZ

**Smoothing the Effects of Renewable Generation on the Distribution
Grid**

A thesis submitted in satisfaction
of the requirements for the degree of

MASTER OF SCIENCE

in

ELECTRICAL ENGINEERING

by

Paul Naud

December 2014

The Thesis of Paul Naud
is approved:

Professor Patrick Mantey, Chair

Professor John Vesecky

Professor Stephen Petersen

Tyrus Miller
Vice Provost and Dean of Graduate Studies

Table of Contents

List of Figures	iv
List of Tables	v
Abstract	vi
1 Introduction	1
1.1 The Grid	1
1.2 Photovoltaic Generation	3
1.3 Smoothing Variability	7
2 Methods	11
2.1 Model 1	12
2.2 Model 2	14
2.2.1 Safety Concerns	25
3 Results	26
4 Discussion	32
4.1 Future Work	36
5 Conclusion	37
Appendix	39
References	47

List of Figures

1	PV Cell Efficiency	4
2	PV Cell Outputs	5
3	PV Power Output on a Good Day	6
4	PV Power Output on a Bad Day	6
5	Energy Smoothers	7
6	Grid Example	11
7	Simplified Configuration of Control	12
8	PV Power Output for a "Good" Day	13
9	PV Power Output for a "Bad" Day	14
10	Simplified Configuration of Flywheel Model	15
11	Simulink Model of Dual Motor Configuration	15
12	Torque Visualization	18
13	Frequency Response of the Flywheels	21
14	Step Response of the Flywheels	23
15	Flywheel Subsystem Model	24
16	Generator Outputs for On/Off Supply	26
17	Generator Outputs for Noisy Supply	27
18	Final Generator Outputs for a "Good" Day	28
19	Final Generator Outputs for a "Good" Day (Zoom 1)	28
20	Final Generator Outputs for a "Good" Day (Zoom 2)	29
21	Final Generator Outputs for a "Bad" Day	31
22	Final Generator Outputs for a "Bad" Day (Zoom)	31

List of Tables

1	Cut-off Frequencies	22
2	Efficiency on a "Good" Day	30
3	Efficiency on a "Bad" Day	32

Abstract

Stabilizing Solar to Grid

by

Paul Naud

Renewable electrical power sources offer a clean form of energy that is essential for the future. In areas with "good" sun exposure (insolation), like Santa Cruz, photovoltaic (PV) power can meet a significant portion of electrical energy demands. However, PV power is variable, and particularly as a result of weather phenomena. This thesis discusses options for smoothing the output of PV production of residential customers by use of a flywheel system. An economic proposition is also suggested in the context of electrical energy rate schedules that could provide cost incentives needed for this smoothing system and make it commercially viable. Using these parameters, it is shown that flywheels used in this capacity are not the correct solution due to the constraints outlined within this thesis.

1 Introduction

With the depletion of fossil fuels, we are fortunate that economical renewable sources, such as wind and solar (using turbines and photovoltaic generators respectively) are now available and affordable, and that these can provide significant energy to meet user demand. However, these renewable electric generators are volatile in their power output [3, 13, 18, 27]. With the growing presence of renewable generators on distribution feeders, storage systems and smoothing techniques are needed to reduce the volatility [2, 12, 13, 19, 20, 21, 28]. Reducing the volatility of renewable generation in distribution feeders would encourage further growth in the portion of energy coming from renewable sources. Focusing on technologies that a consumer, such as a home owner, could purchase and use to smooth their effect on the grid is the primary focus of this work. Due to this constraint, size and cost play an important role in selecting a smoothing option for consumer adoption.

1.1 The Grid

The power grid is significantly invested in technologies that are not amenable to changes or disruptions. When originally conceived by Thomas Edison in 1879, generation plants produced DC voltage with very limited range [10]. This system had an output of 110 V and could supply up to 30 kW of lighting for 59 customers in one square mile area, about 2.4 km at the furthest distance. Edison's competitors, however, pushed AC generation due to the significant problems in DC, particularly range and I^2R losses. AC gained more ground when William Stanley introduced a commercial transformer in 1885. Using transformers, generated AC voltages can easily be increased, proportionally decreasing current, while preserving power. The resulting transformation to AC and its significant reductions in I^2R transmission line losses increases transmission distances and capacity, minimizes line-voltage drops [10, 22]. AC systems reduce right-of-way requirements per MW transfer, and overall operating cost of transmission [10, 22]. In 1888, Nikola Tesla described the idea of two-phase induction and synchronous generators that led to the development of the first three-phase line in Germany, transmitting 12 kV at distances up to 179 km.

Westinghouse Electric Company, founded in 1886, acquired the patents of Tesla and started the development of AC power. This led to the first single-phase AC line in the US by 1889, operating in Oregon, between Oregon City and Portland (≈ 21 km at 4 kV). By 1893, California had the first three-phase 50 Hz line in the US, transmitting 2.3 kV at distances of 12 km, securing the three-phase induction motor conceived by Tesla as the new generator. The US later converted to 60 Hz as the standard frequency, allowing for smaller generators with the same ratings.

Currently, generation in electrical utility systems occur primarily at (large) nuclear, hydro-power, gas turbine, or coal power plants [10, 22]. The power plant voltage levels are typically generated around 11-25 kV, with high current outputs, and must be transmitted along large distances (>100 miles) since they are typically in remote locations due to physical size, type of resource used for generation (hydro), and safety (nuclear meltdown possibilities, coal pollution, etc.) [18]. With these multiple generation locations, power flow problems arise due to interactions between them as they individually work to maintain voltage and frequency. Automation of power plant control (LFC) addresses these issues.

Standardization of transmission voltages were introduced to allow manufacturers to build equipment for utilities, who could then mix-and-match from any vendor. The US standards, with 10% tolerance, are: 69, 115, 138, and 230 kV for transmission lines operating in the high voltage (HV) region, 345, 500, and 765 kV for transmission lines operating the extra high voltage (EHV) region. After transmission, the voltage is stepped down at a substation for distribution to customers.

Substations receive power via transmission lines from the power plants, convert the voltages to distribution standards, and supply power to the surrounding area. To improve reliability, they often have connections to other substations, with multiple pathways. This ensures that if one pathway used to connect the substations is down, there is still another path for the substations to remain connected. However, older

systems may not have multiple pathways and often contain points of failure [10]. Developed for the same reason as transmission, the standards for US distribution, with 10% tolerance, are: 2.3, 4.160, 12.47, 13.800, 25 and 34.5 kV. These voltages are determined by the power requirements of the area being fed. Higher density areas will typically have a higher distribution voltage to avoid sags, handle high load capacity, and extend distances to cover larger service areas. Lower density areas tend to use a lower distribution voltage since the load is comparatively smaller [10].

Each substation transmits power via multiple distribution lines, or feeders, each containing three phases, with one line per phase. The feeders then extend in multiple directions from the substation to service the area. Along the feed paths, transformers attached to one, or multiple phases, step down the voltage to feed a load (i.e. a house, business, or other large power consumer). The load voltages are standardized, with 5% tolerance, to: 120, 208, 240, 277, and 480 V, which are determined based upon the load being serviced [7]. Typically, homes are classified in either the 120, 208, or 240 range, depending on how much energy is consumed by the customer, while the 277 and 480 are left for industrial consumption. As the power flows down the feeder, loads along the path will receive different voltages due to the other loads on the line, but still within the tolerance and thus not noticeable to the consumer. Should a load at the end of one of these feeders become significantly large, the voltage along the line may sag, causing the feed voltage to dip under the required tolerance. With the constant fluctuation of the voltages due to disturbances along the distribution lines, the power flow and maintenance of its voltage profile becomes a nontrivial problem.

1.2 Photovoltaic Generation

Photovoltaic energy is a renewable source that customers can use to supply power for their homes and save on their energy bills. A PV system allows a customer to reduce the use of power from a utility and replace it with power being generated from their PV array. The generated power is around 16 Watts per square foot (W/ft^2)

(and only around 20% efficient) [16]. Most PV panels are sized for 200 to 250 W, a physical size of around 12 ft². As seen in Figure 1, the efficiency of PV cells is predicted to improve.

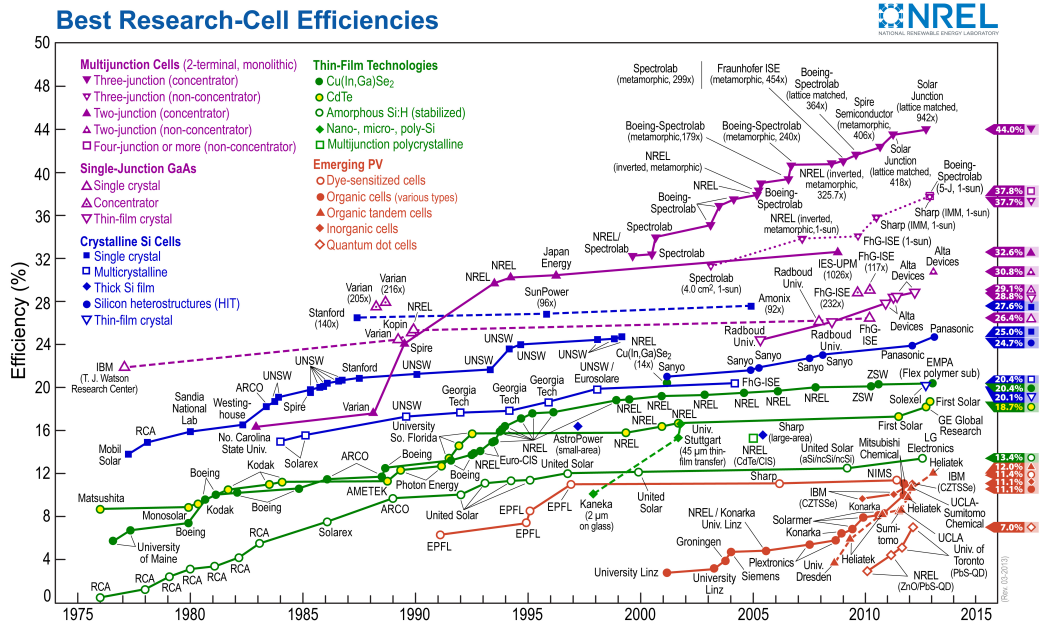


Figure 1: Informative depiction of solar cell efficiency since their development as a commercial product [15]. A larger image can be seen in Section 5.

PV converts solar energy to electrical energy via the photoelectric effect in photocells (PV cells). The photoelectric effect creates a voltage and current from the energy displaced during the absorption of photon energy, causing expulsion of electrons. By placing multiple PV cells in an array with parallel branches of PV cells in series, a stable voltage output can be achieved (Figure 2). However, the current can vary since each photocell will emit different amounts of current based upon the amount of sunlight absorbed, causing output power to vary with changes in solar radiation impinging on the panel cells generation [24, 25, 26].

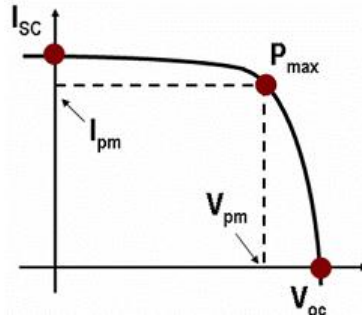


Figure 2: IV curve describing PV cell conversion.

The variation in power output arising from the varying current results from the dynamics of insolation, or the amount of solar energy received by the panel cells. Under ideal conditions, the sun's solar radiation at any location and time of day and day of the year can be predicted. This prediction also depends on the angle of the sun's rays relative to a given panel. When the sun is perpendicular with respect to panel, the amount of energy received (all other conditions equal) is at the maximum (P_{max} in Figure 2). Since the PV panel is not 100% efficient, the remaining solar energy not converted to electrical energy becomes heat. This local heating causes the PV cells to breakdown, which lowers the efficiency of the PV panel over time. If kept in a cool environment where the cells can dissipate the heat, the lifetime of the PV panel can be increased. Based on the parameters of a specific installation, the amount of energy from a PV array can be estimated for ideal conditions. Weather and other atmospheric phenomena will reduce the amount of solar energy reaching the panel and consequently reduce its output. Figure 3 is the output measured for the "good" conditions (near ideal), while Figure 4 is the output measured under "bad" conditions, when weather is causing significant variations and reductions in the solar energy reaching the panel. This output will be used for evaluation of the proposed smoothing under these (representative) poor conditions.

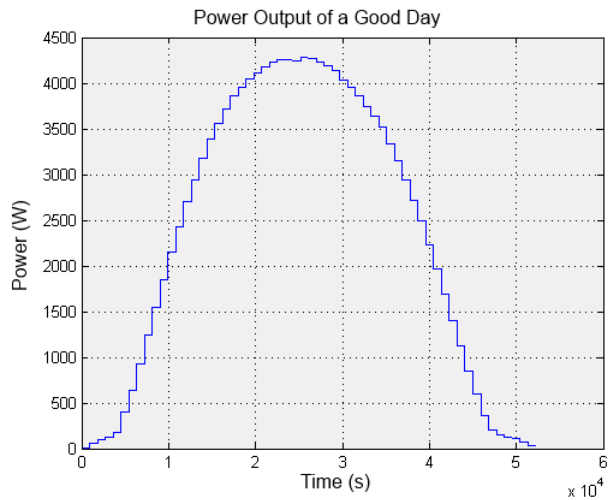


Figure 3: Example of PV power output on a "good" day (in 15 minute intervals).

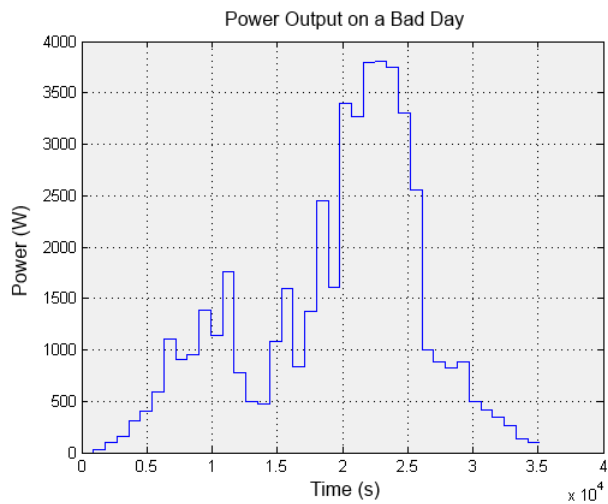


Figure 4: Example of PV power output on a "bad" day (in 15 minute intervals).

The data is gathered from the inverter, which converts the DC from the PV array into AC to transmit along the distribution lines [3]. The inverter creates an AC waveform with a voltage slightly higher than that of the power received at that location from the distribution grid. This forces the energy to flow from the inverter to the grid. A concern about safety must be addressed for the protection of utility workers. If the distribution grid is not supplying power (due to a downed line or other system failure), and thus requires repair, the system must prevent renewable generation sources from feeding energy into the line. This is accomplished within

the inverter design. The inverters approved for grid-tied use will only supply output when they detect that there is an appropriate voltage on the distribution line to which they are connected.

1.3 Smoothing Variability

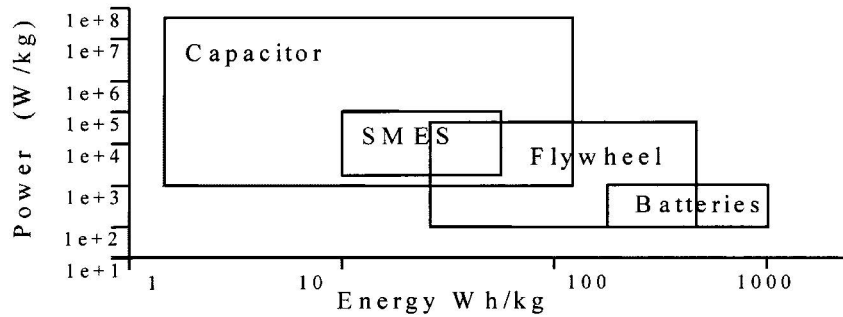


Figure 5: Graphical depiction of different energy storage used on the grid [19].

When generation fluctuations are significant, the grid will be stressed to respond to these and maintain the voltage and frequency of the service [19]. When alternative generation such as PV is connected to the distribution grid, variations in this generation compound the problem already facing the grid as loads vary along the distribution feeders. There are alternative ways to smooth a variable source, as seen in Figure 5, depicting the various options available: inverters, capacitors, SMES, batteries, and flywheels.

Inverters can be used for smoothing and are required for any grid connected PV [3, 6]. The inverter operates by taking the DC source and "inverting" it into an AC source. Grid-tied inverters perform voltage regulation, and produce a smooth voltage waveform from the variable DC source [11, 17]. The inverter uses buck/boost converters to regulate the output voltage based on an input voltage, providing a virtually constant voltage. The voltage is virtually constant as the buck/boost converter alternates a pulse-width modulated (PWM) signal into two MOSFETs connected to the positive line and ground. By varying the PWM percentage to each MOSFET, the voltage is controlled to a desired output value. Using this technique

works fairly well, providing the desired voltage while the current varies with the power received from the DC (e.g. PV array) source [17]. There is an upper limit for the current, beyond which the inverter will not operate. The system will also not operate if the input voltage has too much variability since a buck/boost chip has an input range of voltages that it can regulate. Since the inverter is required, it cannot be removed from the grid-tied system. However, providing a smoother input into the inverter can assist the smoothing needs.

Another smoothing option is the use of capacitors. They work by accumulating positive and negative charges on separate, parallel plates, and may have a dielectric material separating the plates. [19]. For increased capacitance, the plate spacing and/or size must be increased; or a different dielectric material used. On the grid, the capacitor provides short-term DC storage units [19]. When used in conjunction with other generation elements on the grid, they provide assistance in voltage sags and momentary interruptions for distribution lines by adding their stored energy to the line, increasing the voltage temporarily [19]. Capacitors are used to produce reactive VARS, balancing out the inductive VARS that come from inductive (motor) loads, and thus move the power factor closer to 1.0. This reduces the current and lowers the voltage drop on the line. The size of the capacitor changes based upon the voltages on the line. The larger the voltage, the larger the capacitance needed, which increases the overall size of the capacitor. These capacitors are actually already in use with inverters to give a small amount of smoothing. However, the smoothing we are attempting to achieve would require much more capacitance than achievable within an inverter. Therefore, despite the usefulness of capacitors, they have been eliminated as an option for smoothing a consumer's PV system.

Superconducting Magnetic Energy Storage (SMES) is also used on the grid and is one of the first proposed energy storage systems to be used, dating back to 1970 [19]. SMES systems are attractive because they have fast response times and high efficiency ($\approx 95\%$) [19]. The system stores energy in a magnetic field generated by a

DC current flowing through a superconducting coil, storing the energy as a circular current. This allows the SMES virtually instantaneous responses (anywhere from a period of a fraction of a second to several hours) to power demands [19]. However, an SMES unit requires a large superconducting coil kept in temperatures below 100°K. In order to produce the amount of energy required to achieve the required temperature, it would need a cooling system that may take more power than what is generated by a solar panel [4, 19]. The cost for this could also be more than what would be saved by having a PV system, which eliminates this as a viable form of smoothing PV for consumer use.

Another cost-effective option for energy storage is the use of batteries. Today, batteries are being used to achieve some smoothing on consumer PV systems [2]. Battery systems are made up of a series-connected branch of low voltage modules, which are then connected in parallel to multiple branches to achieve the desired voltage. They function somewhat similar to a capacitor, accumulating positive and negative charges between parallel plates, but contain chemicals between the plates that react to the charges. Batteries undergo an internal chemical reaction when charging, and deliver the absorbed energy when the reaction is reversed [19]. This allows batteries to have high energy density, high energy capability, round trip efficiency, cycling capability, long life spans and low initial cost [14, 19]. A drawback of using batteries is that, due to the chemical reaction, they cannot supply high energy outputs for a long period of time. They are also plagued with deficiencies in the manufacturing process, resulting in about 20% of production to be faulty [1]. Certain types of batteries may contain chemicals that are harmful to the environment and people, should a leak occur. Batteries also have a lifespan problem, which is around 5 years for deep cycle versions [1]. Due to these faults, batteries are not considered as a viable smoothing option.

Finally, the use of a flywheel presents an option for smoothing. A flywheel can quickly respond to voltage changes, and requires few parts in the design [1, 8]. There are

two types of flywheel designs that are used for this purpose: high speed and low speed [4, 20, 21, 28]. High speed flywheel designs are physically smaller systems, while low speed flywheel designs are larger [8]. The advantage to the high speed system is a low initial power required to start storing the energy. The advantage to a low speed version is the cost of the system; however, power losses are increased due to the initial power required to move such a large mass up to angular speed [21]. Both systems have the advantage of working in ambient temperatures, which means little to no cooling is required. They can also correct a power change within 2 cycles, and do not have the deficiencies that plague batteries [1, 21]. Either high or low speed will work for smoothing and the choice may involve other factors and customer preference. Using either system with a renewable source, the energy will be smoothed before input to the inverter. Models have been developed that simulate the best way to use and control a flywheel designed system to allow for smoother outputs [9].

on the distribution lines with respect to the per unit value of the line (they have been exaggerated in Figure 6). While in *run mode*, the introduction of a disturbance effects the pie charts percentages, demonstrating load imbalances, which in turn allows users to visualize the power flow on the grid. Not shown in Figure 6 are animated arrows that give speed, direction, and amplitude of the power flow in steady state. The size and speed of the arrows are proportional to the percentage on the lines they would travel along. Unfortunately, *Powerworld 16.1* only shows a steady state system with the current license and cannot be used to illustrate the effects a volatile source can have on the power flow of a distribution system.

In order to evaluate the effects of an electrical generation source in the distribution grid, data from an existing PV array is used. Data from a customer's 5 kW system, with data from the inverter, on both DC in and AC out, measured every 15 minutes was used. Using their existing PV array data as the input, the smoothing achieved and the overall efficiency of flywheel systems was simulated.

2.1 Model 1

Known as the control model, this model uses a PV array connected through the standard configuration when tying to the grid. The PV is fed into an inverter to feed energy into the distribution system. A simplified depiction of this system is shown in Figure 7.



Figure 7: Simplified overview of the control system.

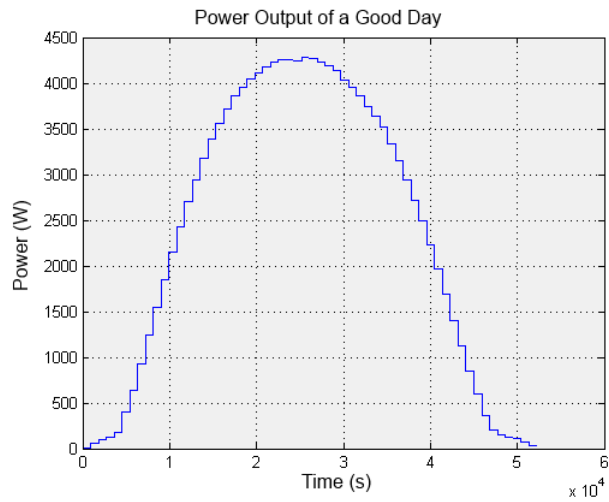


Figure 8: An example of PV power output during a "good" day (15 minute intervals).

This reference data for a "good" day production, taken every 15 minutes, shows power output of the PV array, where the output variation is dependent upon time-of-day and corresponding sun angle. (Figure 8). Since the data is in 15 minute intervals, a zero-order hold effect is seen, meaning that the last value given is held for 15 minutes until the next value is received. While this data is not ideal, in that with the sampling interval of 15 minutes it has lost the more dynamic variations of the PV array output due to minor changes in atmospheric or other local conditions, it is the best data we had for representing what a PV array produces under near ideal conditions.

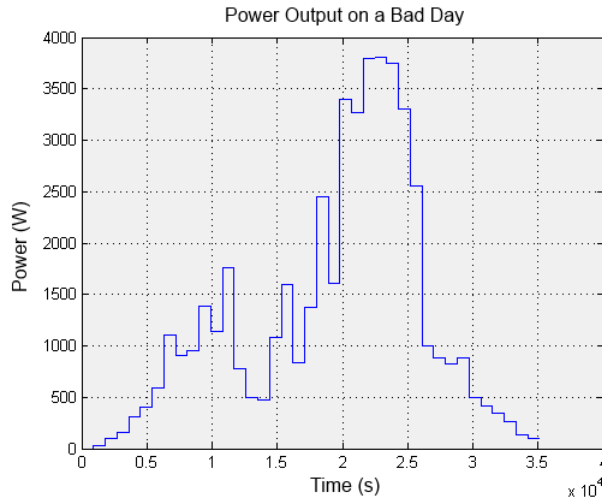


Figure 9: An example of PV power output during a "bad" day (15 minute intervals).

While simulations of the effects of flywheel smoothing for the "good day" data is interesting, the value of the smoothing is more apparent with the data coming from the array on a "bad" day where changes in weather or local atmospheric conditions result in significant and unpredictable changes in the output of the array (Figure 9). The data came from the same PV array as the reference for a "good" day, but under significantly different conditions including both weather and day of the year.

2.2 Model 2

To address the smoothing option, a design using a flywheel with two motors was examined. This system takes the energy from the PV array and feeds it into a motor. The motor has a flywheel attached to the mechanical shaft, which is also attached to the shaft of a generator. Since the generator is only fed from the flywheel, it forces all the energy created by the PV array to be filtered through the flywheel (Figure 10). The advantage of this design is that all the power generated is converted into rotational energy, with corresponding inertia. This inertia smooths the transitions of the output. However, there will be some loss of overall energy due to friction, motor resistance, and windage (turbulence).

the generator output will have a voltage output dependent upon the torque input. Therefore, the voltage will not be as constant as the PV array gives and will cause slight changes in the power output (discussed in Section 3).

For developing the simulation, the simulation of the motor subsystem was the first step. To appropriately generate the current and voltage from the power data, and to ensure accuracy, the data was read directly from the file and stored as an array over time. Using designed conversion blocks for current and voltage from Matlab, the data was fed into the DC motor's armature current and field voltage, respectively.

In SimPowerSystems, there are numerous types of generation sources to use. Some of these have built in controls, while others allow for a more personalized design. An excitation system is also available for all generation systems. However, a simple "DC Machine" block was chosen for the motors of the system since it met all the requirements for simulating the system. The DC Machine allows the user to select the internal resistance, inductance, and operating voltage, while transmitting outputs of angular speed (ω_n), the armature current (the current associated with the torque output), the field current (the current flowing through the windings of the motor), and the electrical torque. The DC Machine also allows the user to have torque inputs, or speed inputs to power the motor and change the mode (motor or generator). These values help produce the correct output power and verify that the correct input is being produced on the motor. The angular speed is the data used to feed the flywheel model, and the flywheel feeds energy into the generator, but also back feeds into the motor.

To use the DC Machine model, there are several parameters to choose. T_L of the model is the mechanical torque applied to the motor (If left disconnected, the motor does not act accordingly and gives us an incorrect output power). To feed the current from the PV data, a "Stair Generator" from the simulink library was used. This creates the zero-order hold on the 15 minute data discussed earlier (Figure 8).

This output is fed into the "Current Conversion" block, which feeds into the DC Machine's armature current input. However, if connected directly to the armature input, an error would occur and will not allow the simulation to run. To avoid this error, MATLAB suggests a large resistance placed between the input and ground; hence the large resistor on the output of the conversion block (Figure 11).

The DC Machine also needs a voltage input to operate. The data taken from the PV system has the measured voltage, and since we want to simulate as close to possible a PV system connected, a "Voltage Conversion" block was used and fed directly into the field coil of the DC Machine.

Once the motor is set, a flywheel block is created. Since the flywheel block does not exist in Matlab, a subsystem block was used. The subsystem block allows the user to define inputs and outputs to the block that will interact with the higher level system. Starting from physics, the flywheel is fundamentally a mechanical device and stores energy in its angular momentum. Following linear motion (Equation 1), we know that force (\vec{F}) is mass times acceleration, or the derivative of velocity (\vec{v}). This equation can be further simplified by substituting mass times velocity as linear momentum (\vec{p}), resulting into the definition of linear motion. By using this substitution, the total net force is defined because linear momentum is a vector that defines all the velocities exerted within the mass.

$$\vec{F} = \frac{d}{dt}m\vec{v} = \frac{d}{dt}\vec{p} \quad (1)$$

For a linear system, the energy is stored through kinetic energy (E_k), which defines the energy contained within the object due to motion (Equation 2).

$$E_k = \int_0^t \vec{F} \cdot d\vec{x} = \int_0^t \vec{v} \cdot dm\vec{v} = \frac{1}{2}mv^2 \quad (2)$$

To transform from linear to angular involves taking the cross product of some length vector (\vec{r}) to the linear force (F), which produces a rotation. This works in the same

way of pushing or pulling in linear force, but pivoting around a fixed point (Figure 12). The resulting transformation is defined as torque ($\vec{\tau}$), which allows for the translation of linear energy into angular energy.

$$\vec{\tau} = \vec{r} \times \vec{F} \quad (3)$$

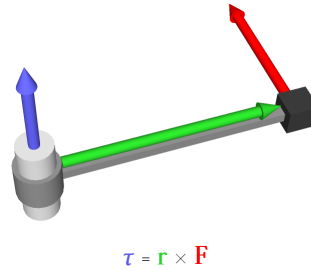


Figure 12: Visual interpretation of torque definition.

Similarly to how we simplified linear force, we can define the net torque (τ_{net}) in terms of angular momentum (L) (Equation 4). By adding the momentum to the system, it forces the system to apply an opposing force to slow it down. This can be experienced when applying the brake on a moving vehicle. When braking, the vehicle slows down depending upon the amount of force applied to the brake. This translates to a force vector applied in the opposite direction of torque in an attempt to decrease the generated torque from the rotating mass, or the rotors of the vehicle. The mass of the rotor is much less than that of the entire vehicle, and may stop, causing a skid, while the vehicle continues moving. This is because the stored energy in the linear momentum of the vehicle is too great to overcome immediately.

$$\tau_{net} = \frac{d}{dt} \vec{L} = \frac{d}{dt} (\vec{r} \times \vec{p}) \quad (4)$$

Angular momentum is how a flywheel stores energy and can smooth a system. Applying the same techniques, kinetic energy can be translated to angular energy (E_L), or the sum of kinetic energies due to the rotation of the object (S) around the axis

through its center of mass (Equation 5).

$$E_{\angle} = \int_S E_k = \frac{1}{2}\omega^2 \int_S r^2 dm \quad (5)$$

Angular kinetic energy in terms of a flywheel is further simplified using the moment of inertia (J). This is calculated based on the equivalent mass of an object rotating about the object's balanced center of mass (m), where r is the moment arm, or distance to the equivalent lumped mass (Equation 6). Solving the equation results in a large factor contributing to the energy. Should we change the radius, the moment will square the effects on the angular momentum. This means that with the same mass, but an increase in the radius, the moment is increased. To experience this property, take a yo-yo and rotate it along a fixed string length. If the length is increased, the yo-yo requires more energy to rotate at the same speed as before. If you decrease the length, it takes less energy. The difference in the amount of energy required is the square of the radius since the mass was not changed.

$$J = \int_S r^2 dm = mr^2 \quad (6)$$

From the definition of the moment of inertia, Equation 5 can be simplified further (Equation 7).

$$E_{\angle} = \frac{1}{2}\omega^2 \int_S r^2 dm = \frac{1}{2}J\omega^2 \quad (7)$$

This describes how a flywheel operates. However, a flywheel can be decomposed further as having two operational states, either "charging" or "discharging." A flywheel's operational states are dependent upon its configuration in the system, either as a parallel source, or a series filter. While in parallel, or used as a back-up source, the system stores energy from another source. If that source raises or drops too quickly, the flywheel can be used to absorb the high rise, or discharge to avoid the quick drop. This means that our angular velocity ($\omega(t)$) will be contained in one of these states at any given time (Equation 8). When placed as a series filter (as in the

system proposed here), it is in both states simultaneously, receiving and delivering energy. This means that the flywheel is continually charging, while also discharging.

$$\omega(t) = \begin{cases} \omega_{max} & t \leq T \\ \omega_{max} e^{-\frac{K_0}{J}t} & t > T \end{cases} \quad (8)$$

Analyzing the parallel system, the first state is defined as the charging state, which is absorbing all the energy being sent until full ($\leq T$). For the discharging state, there exist an exponential decay of energy defined by the torque conversion factor from mechanical to electrical energy (K_0) divided by our moment of inertia, whenever we have more energy than possible ($> T$). However, this system would require a controller to analyze the source quickly enough to respond in time, which may still cause transients to appear due to computational latency.

Using T , we can determine the maximum nominal power of the flywheel (Equation 9). The power will change based upon the region it is being discharged in, so a piecewise representation is still needed for the parallel case. When the flywheel reaches the exponential region, the power will be the derivative of the energy with respect to time, where η_{fw} is the efficiency of the flywheel [1].

$$P(t) = \begin{cases} \frac{E}{T} & t \leq T \\ \eta_{fw} \omega_{max}^2 e^{-\frac{2K_0}{J}t} & t > T \end{cases} \quad (9)$$

Typically, a flywheel's efficiency is high (between 95% and 98%), which is why this particular system is being examined [1, 4]. The reason for the high efficiency is because the system only losses energy in friction, motor resistance, and turbulence. However, for a parallel system, a possible problem is amount of time they can output their rated capacity. According to the datasheets, flywheels can output their stored energy between 10 and 20 seconds, which may or may not be enough time to effectively smooth the variability of a PV panel [1, 9]. Although, some results conclude that the flywheel discharges at 10-20% of total capacity per hour, but does not explain the configuration of this type of flywheel system [4].

The configurations discussed in current literature use the flywheel as a parallel source. The model developed in this thesis uses the flywheel in series with the output power, which causes the flywheel to act like a low pass filter, smoothing the output of the system. The energy losses of the filter system compared to the PV source will be dependent on the size of the flywheel and motors. Large motors and flywheels will react slowly to any changes, resulting in a higher initial power to start the flywheel system and a lower cut-off frequency, but supplying increased smoothing (Figure 13). Likewise, with motors and flywheels too small, the system will smooth, but the effects of smoothing may be unnoticeable on the output system due to the higher cut-off frequency. It should be noted that the PV output data being used, which is data averaged and sampled every 15 minutes, does not contain the actual variation generated from PV arrays. However, it was the only data available for use in this study. From the frequency response, it is seen that high frequency variations in the output from the PV array will be attenuated.

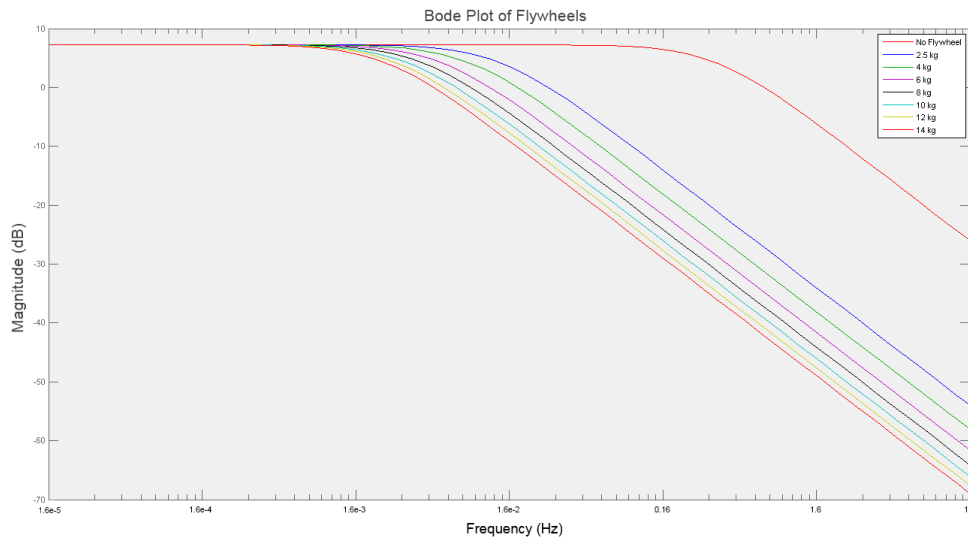


Figure 13: Bode plot of the effects the flywheels have on the frequency response of the system. Larger version can be seen in Section 5.

Flywheel Size (kg)	Cut-off Frequency (Hz)
Null	7.958×10^{-1}
2.5	3.18×10^{-2}
4	1.99×10^{-2}
6	1.33×10^{-2}
8	9.9×10^{-3}
10	8×10^{-3}
12	6.6×10^{-3}
14	5.7×10^{-3}

Table 1: The theoretical cut-off frequencies for the different flywheels.

Along with the frequency response, a step response per flywheel is analyzed (Figure 14). This demonstrates the rise time of the multiple flywheels and is used for system behavior. Theoretically, all the flywheels should represent an under damped system, with longer rise times attributed to larger sized flywheels (higher J) but should never exceed the final value. This implies the moment (J) contributes to the behavior of the system. For higher moments, a longer rise time exist, and vice versa. This holds true since the a larger momentum (contributed by the larger J) would require more energy to change. Since energy is defined as the work over time, longer times are required for larger moments.

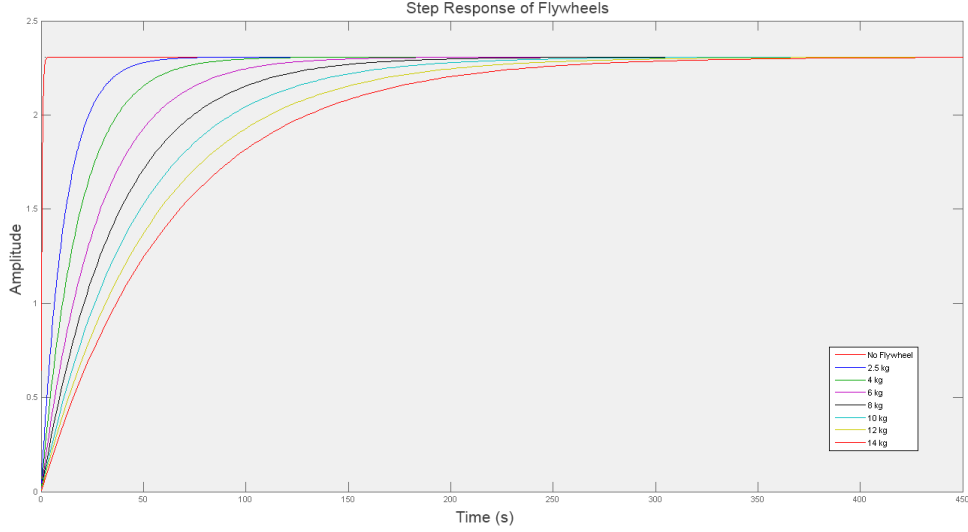


Figure 14: Step response of the different flywheels. Larger version can be seen in Section 5.

Using the fundamental equations, our generated outputs are ω_{mn} from the motor and ω_{gn} from the generator. In Figure 15, there are two gain stages in the flywheel subsystem, one for feedback to the first motor, and the other to put the second motor into generator mode. For the simulation blocks to act appropriately, a negative input into the DC Machine will put the block in generator mode. Alternatively, sending a positive value will have the block act as a motor. The absolute value will also need to be less than 1 per unit value, defined within the DC Machine properties, in order for the generator to act appropriately. The flywheel subsystem requires the following inputs to meet all the requirements: radius of the flywheel (r), the mass of the flywheel (m), the rotational speed from the motor ($\omega_{mn}(t)$), and the rotational speed from the generator ($\omega_{gn}(t)$). Using Equation 7, J is created using the subsystem by taking r and squaring it, then multiplying r^2 and m together. Next, it takes ω_{mn} with a gain of 0.02 ($1 - 0.98$ to depict the highest efficiency of a flywheel) and divides it by a motor constant (K_0), which scales the size of the motor. Scaling the motor can also be done within the DC Machine block, but for simplicity, was done in the flywheel system. The product is then multiplied with $-J/2$ before

multiplying again into ω_{mn} to become the input to the generator. The subsystem also allows the generator feed ω_{gn} to be sent back to the motor while going through the same calculations to account for the flywheel between them. The absolute values of ω_{mn} and ω_{gn} must be the same since the flywheel will act upon both DC Machines equally. This assumes a rigid shaft connecting the motor, flywheel, and generator together.

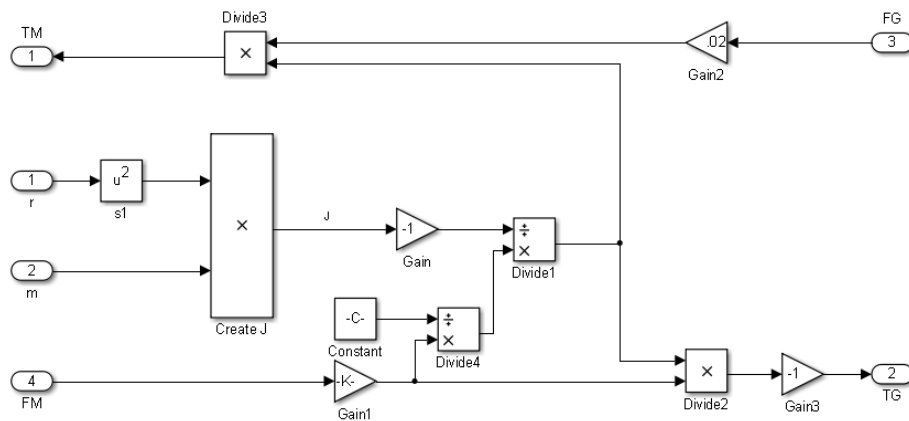


Figure 15: Subsystem block used to simulate the effects of the flywheel in the system.

Before looking at "good" and "bad" day simulations, simpler inputs will be used to view the responses of system. Initially, the system will simulate an ideal source that is on or off with a fixed amplitude. This will run over a fixed amount of time to verify the theoretical responses, which should indicate a larger flywheel having a slower response time. Afterwards, the inputs will be changed to the PV measured data of voltage and current. To appropriately simulate the system, a time scale of 1 millisecond was used. The simulation should demonstrate the effects of different sized flywheels on the power output to be smoother, with larger flywheels providing greater smoothing. Since the data is not changing rapidly enough, white noise will be added to the measured data to simulate the volatility of PV. Due to simulation constraints, this will be shortened over time, but should still outline the smoothing abilities of the flywheel system. All voltage and current outputs are measured over a fixed load. Multiplying these together give us the power output of the system, with required scaling since the load does not vary.

2.2.1 Safety Concerns

Since the system has a large amount of weight rotating at high speeds, safety is a concern. In order to determine how safe a particular configuration of the proposed model is, it is necessary to examine how the flywheel is made. Every flywheel developed is put through a series of test to determine the strength of the flywheel and to determine the safety ratings for said flywheel [23]. The flywheel undergoes a stress test to evaluate the maximum allowable parameters for proper design margins. Ensuring these parameters are not breached, installing a monitoring systems for the flywheel during operation is recommended. Monitoring for abnormalities in temperature, vacuum level, and rotational vibrations assists in ensuring smooth operation. The final consideration is the construction of a physical protective barrier between the flywheel and the consumer. Using a non-moving barrier around the flywheel is recommended to avoid any accidental touching of the flywheel during operation. A fully contained system without any additional features, or using pressurized containers and energy absorbers for abnormal behavior increases the safety of a flywheel for consumer use.

To determine how dangerous the model may be, an examination of the speeds the flywheel should produce will determine minimum safety requirements. Since the rotational speed plays a vital role, we look at maximum angular speed (ω_{max} in datasheets), which can be calculated using Equation 10. In Equation (10), σ is the tensile strength, ρ is the density, r is the radius, and s is a safety margin given by the manufacturer in the datasheet [1].

$$\omega_{max} = \frac{s}{r} \sqrt{\frac{\sigma}{\rho}} \quad (10)$$

At the speeds the final model will be rotating, our safety concerns are slightly higher than for a flywheel system running in parallel. In parallel, the flywheel will have a fixed rotational speed of 7000+ RPM, depending on the amount of energy needed for the PV source, while the fixed rotational speed of a system in series will vary in RPM.

Safety should not be ignored and it is recommended follow all safety precautions for flywheel operation.

3 Results

To verify the flywheel operates correctly, simulations based upon a simple on/off switching power supply is analyzed (Figure 16). As expected, the response times increase with flywheel size, proving the simulation is developed correctly.

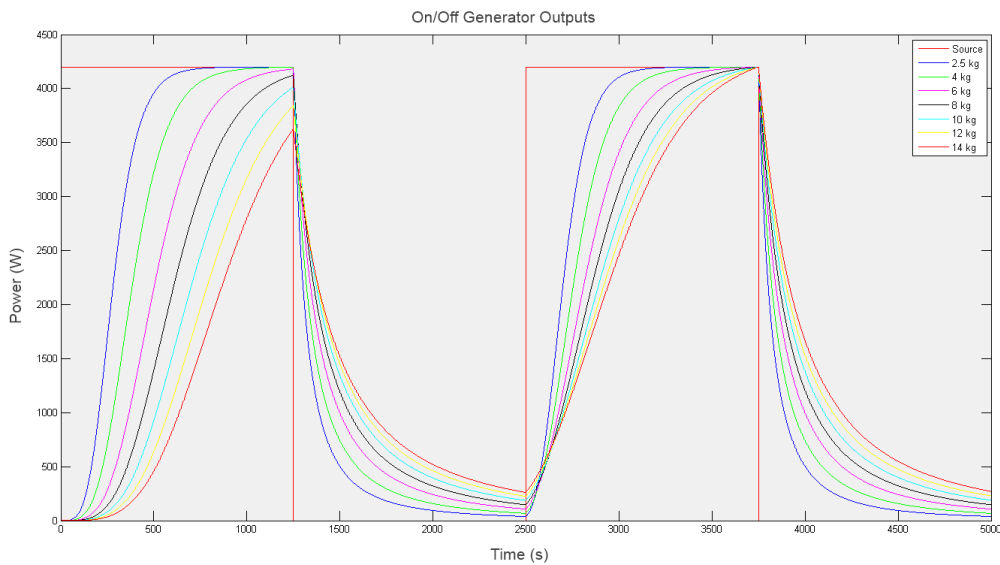


Figure 16: Resulting outputs of the flywheel smoothing system for an on/off supply.

By demonstrating the smoothing for an on/off supply, the system can be expected to work correctly for higher volatility. To analyze this, a second simulation incorporates a noisy supply to represent a higher variable system, but at a much lower time range due to simulation limitations (Figure 17). The system is proven effective since the output is much smoother than the input for any size flywheel and larger flywheels still providing more smoothing.

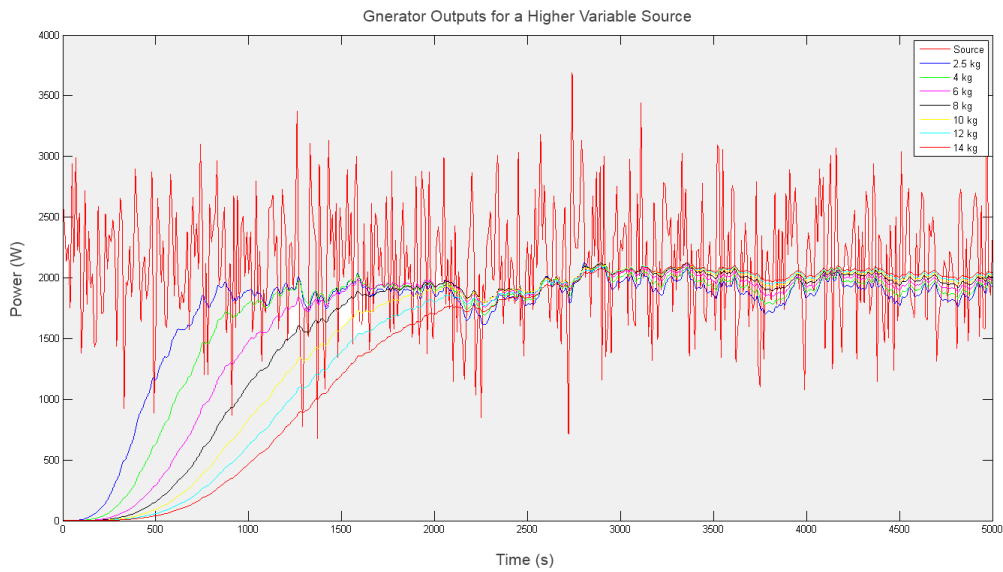


Figure 17: Resulting outputs of the flywheel smoothing system for a "noisy" supply.

Since the system is proven to work, the supply is changed to the existing PV data on a "good" day (Figure 18). As predicted, greater smoothing is achieved by increasing the radius or mass at a cost of response time and average energy. Due to the amount of energy that the flywheel is attempting to change, a larger radius would require more effort for adjustments. A flywheel with a smaller radius rotates much faster for the same energy. This is analytically represented when the moment of inertia (J) has a higher value when the radius is large, requiring more energy to rotate the flywheel, and vice versa (Figure 14). To slightly adjust the moment of inertia, it is easier to change the mass, while fixing the radius. In this thesis, the flywheels were all given a fixed radius of 10 cm, and the mass was varied to experiment with different configurations.

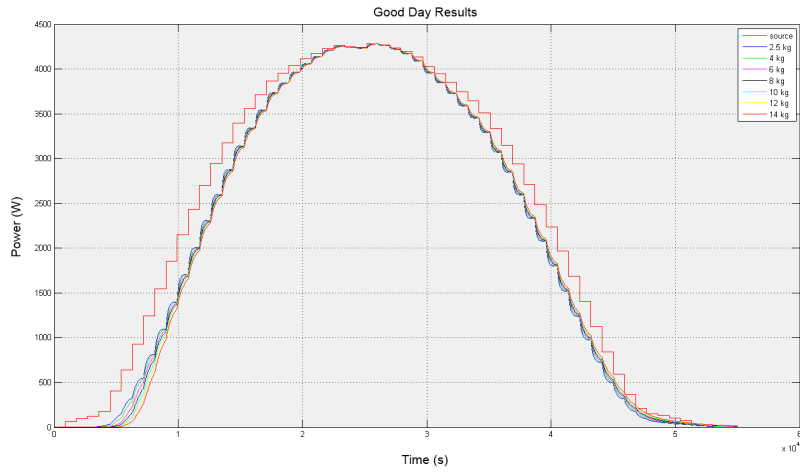


Figure 18: Resulting outputs of the flywheel smoothing system experiencing a "good" day for production. A larger image can be viewed in Section 5.

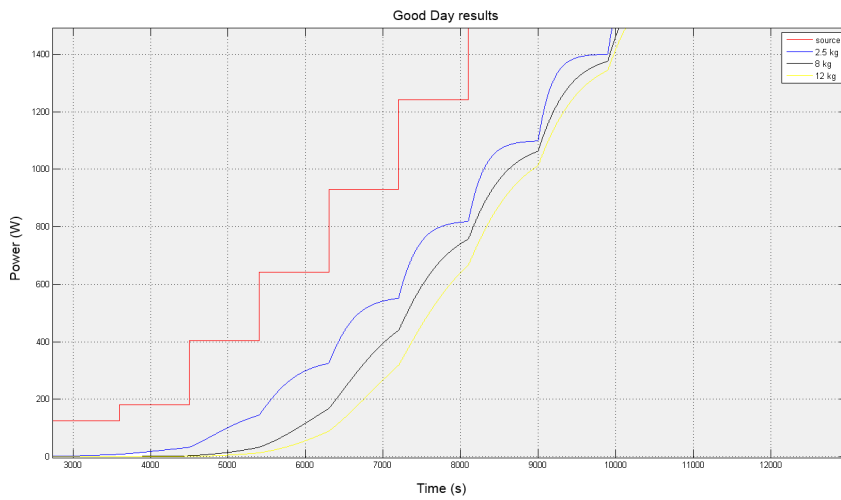


Figure 19: Focused result on rising edge of flywheel smoothing effects on a "good" day of production.

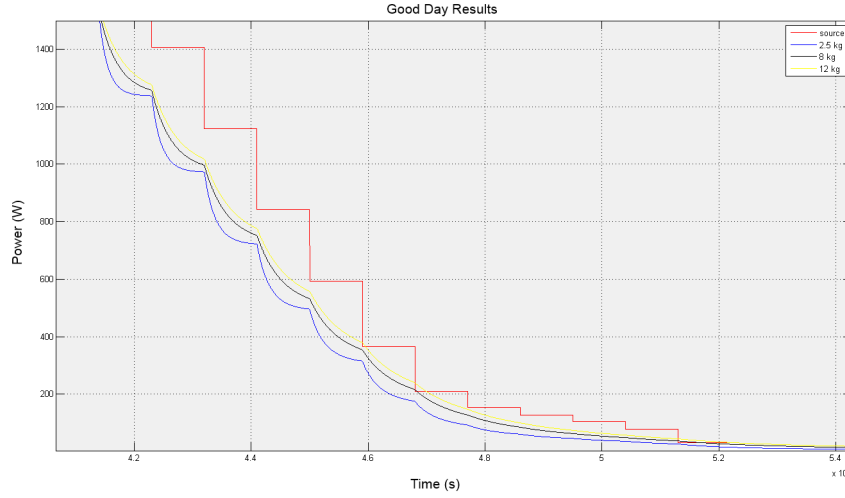


Figure 20: Focused result on falling edge of flywheel smoothing effects on a "good" day of production.

In Figures 18, 19, and 20, there exist a disparity of power output from the input. The PV panel outputs a fixed voltage with varying current. However, the output of the smoothing systems's generator has an output that varies both current and voltage based upon the angular velocity (ω) of the shaft. This dependency causes the power output to store some energy, while also losing some amount from the other factors discussed earlier.

Overall generated power compared to that of the control is found by taking the sum of all the points over the simulation time (T). The resulting sum is then divided by the total sum of the measured PV data and multiplied by 100 to give us the percentage (Equation 11). The efficiency on a "good" day for the different sizes of flywheels are listed in Table 2.

$$\xi = \frac{\sum_0^T \text{Flywheel Power Output}}{\sum_0^T \text{PV Power Output}} * 100 \quad (11)$$

Flywheel Size (kg)	Efficiency (ξ) (%)
2.5	86.76
4	86.72
6	86.66
8	86.60
10	86.53
12	86.47
14	86.41

Table 2: The calculated efficiencies for the different flywheels during a "good" day of production.

The results on a "good" day do not vary as much in efficiency, but prove smoothing can be accomplished with little loss to the unfiltered power output. The differences in the efficiency is due to the initial start. The motor would burn energy attempting to move the flywheel until the energy is enough to overcome the static friction. Once accomplished, but with varying time delays, the flywheel moves and starts the smoothing process. The larger the flywheel, the larger the static friction, thus extending the start up phase. However, in order to truly test the usefulness of the system, "bad" day data must be examined. Figure 21 demonstrates the effects of smoothing on the output of the PV array on a "bad" day, for the different flywheels. Again, the flywheel smooths the output differently, for the different flywheel sizes.

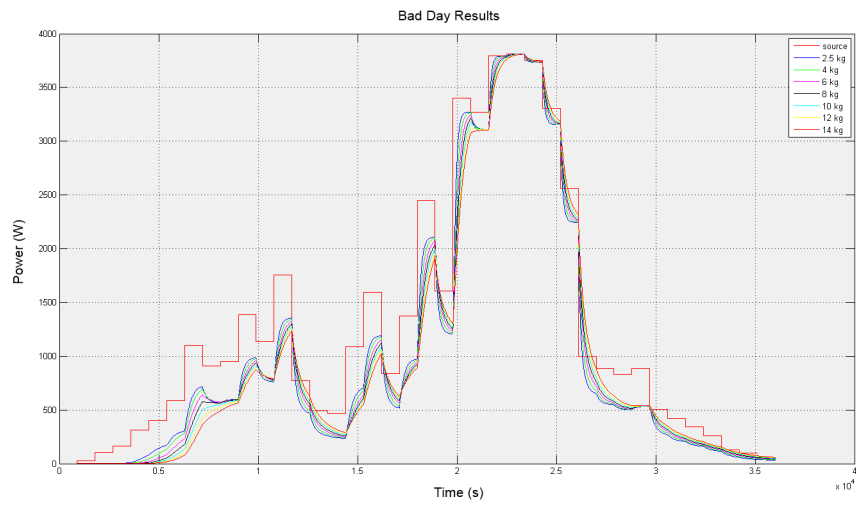


Figure 21: Resulting outputs of the flywheel smoothing system experiencing a "bad" day for production. A larger image can be viewed in Section 5.

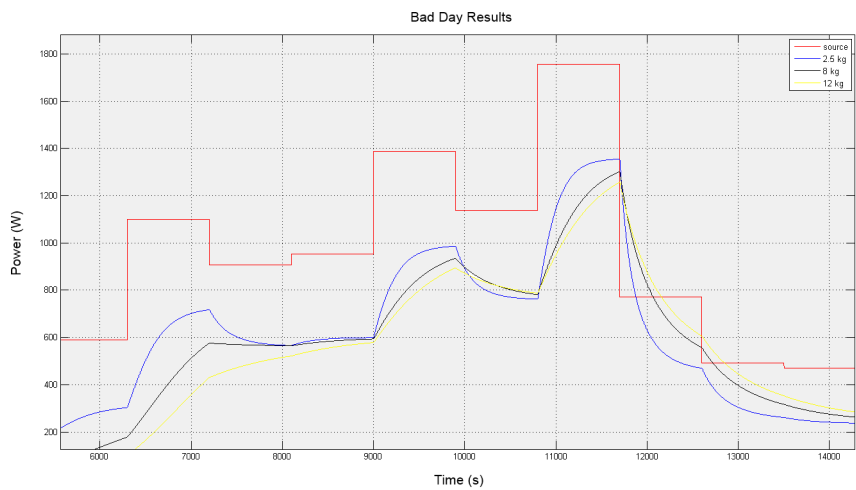


Figure 22: Focused result of flywheel smoothing effects on a "bad" day of production.

On a "bad" day, the charging and discharging rates of the PV array has higher volatility. This volatility is focused through the flywheel, with each flywheel having a different response and peak point from the input source, as expected.

Flywheel Size (kg)	Efficiency (ξ) (%)
2.5	78.50
4	78.25
6	77.94
8	77.65
10	77.38
12	77.12
14	76.88

Table 3: The calculated efficiencies for the different flywheels during a "bad" day of production.

Calculations of the efficiency for "bad" day input data are shown in Table 3. While the smoothing of the PV data from the "good" day exhibits approximately a 13.5% loss, there is approximately a 22% loss in production when smoothing the data from the "bad" day. This decrease in efficiency is due to the drastic changes in angular speed feeding the flywheel, causing frequent adjustments in the flywheels amount of stored energy.

4 Discussion

Several problems were addressed during the development of this model. The initial challenge was to gather real data from a PV system for accuracy. UCSC researchers have a system at NASA Ames Research Center in Mountain View, CA, that has a Max Power Point Tracking (MPPT) system that captures data on generation every five minutes. However, the NASA data seemed too unrealistic for what a residential customer would see as their power output. This is because the NASA system uses only one panel with 170 W output power, measured every 5 minutes, with MPPT, which is rare for customer systems.

Fortunately, inverter data from a customer with a PV system in place solved this problem. This was crucial since the system needs to be tested with typical values in

order to demonstrate the smoothing advantages. While the provided data is for a 5 kW system, other PV systems, even of the same size, may have different patterns of energy production due to different local conditions and orientation, shading, etc. Specific choices of the flywheel system parameters need to consider the site-specific data.

The second challenge was Matlab's SimPowerSystems toolbox. The toolbox lends itself to various useful applications, and can support the creation and simulation of a complex grid system. Unfortunately, there are some caveats to any simulation developed within this toolbox. For instance, without having a time frame established, the system will not run. Furthermore, the time frame itself needs to be fast enough to simulate data accurately. Having anything above a millisecond in this simulation did not show enough of the smoothing because the resolution was not high enough. When the resolution is increased (in this case to a millisecond scale), the number of points can cause the simulation to crash. The "good" day simulation used the 15 minute data over the span of 14.5 hours, which gives us 58 data points. To keep the time accurate, the data was then translated into seconds, which gives us 52,200 data points. Since the simulation is in milliseconds, 52,200 becomes 52,200,000 data points. In order to simulate large data sets such as this, more RAM is required on the computer used.

Once the system was running, understanding how the generator operates in the simulation became challenging. To achieve generation, the torque feed for the generator needs to use a negative gain stage, a constraint within Matlab's block properties and cannot be changed without creating a custom block. Without this, the simulation produced inaccurate outputs. This was due to the configuration of the initial model, which did not invert the feed into the generator. After adjusting the model to simulate the correct configuration, the simulation worked, only too well. The generator produced more energy than available, which meant somehow a system was created that can produce energy out of nothing, violating conservation of energy. Therefore,

a closer examination occurred on coupling of the DC Machines. After examining the system, it was discovered that there was a gain greater than the per unit value of the generator and motor, which meant the simulation would have an energy output greater than 100%. Adjusting the model resulted into a deeper investigation of the Matlab Simulink documentation to make the necessary changes on the coupling portion of the motor. Since there should be no additional energy, the gain must be less than the per unit value for the motor and generator.

The per unit value works by establishing a percentage of power being sent into the DC Machines. For instance, if the gain is too close to 1, the output does not discharge very quickly, which creates a low resistance model based upon the internal resistance of the motor. Too high, and we over-damp the system, giving us basically no input, and therefore, no output. The per unit value can be changed in the system, but the same results would apply. This is done internally to the configuration of the device and implies any gain on ω_n must be less than the per unit value specified for the simulations to work accurately.

While the equations made the development of the system seem straightforward, determining the accuracy of the outputs was not. If we follow Equation 6, then fixing the radius allows for slight changes in the moment of inertia (J). Since the radius is squared for the equation, we can change the mass to see the effects in a more linear fashion (Figures 18 and 21). For this reason, the radius was fixed to 0.01 meters and then changes in J were made by changing the value of the mass. The same load on the output of the generator was used for each simulation to see the effects on the energy output from the generator, and these to be correctly scaled.

Due to the overall benefit from systems that smooth the output from individual PV arrays, and thus reduce the variability of the consumer as seen by the grid, deployment of these systems would require some economic incentives. The consumer does not directly see value when using this system (although without some smoothing

there may be limits to the amount of renewable energy a distribution feeder can accept).

Because the benefits of these go to the distribution system, the costs need to be borne by the utility. As costs of PV arrays continue to decline, more consumers will be motivated to install these arrays at their homes. California passed legislation requiring the state to have 33% of their power grid to rely upon renewable energies by a 2020 goal (SBX1-2 was signed by Governor Edmund G. Brown, Jr., in April 2011) [18]. To accomplish this, major renewable generation plants are in development. However, customers are expected and possibly encouraged by incentives and favorable rate structure to add PV arrays to their homes [18]. Customers can also sell back power to their local utility provider for additional benefits. One major California utility tells customers now that a PV array at their home may provide customers up to 80% savings on their monthly bill [7]. In addition, alternative rate structures from this utility also encourage the selling back of excess energy during times of peak need.

To make this smoothing systems studied in this thesis feasible, the rate structure would need to reward the consumer for this installation of smoothing. Each system must be matched to the site-specific conditions for each customer with a PV array. That is especially true for the selection of the size of the flywheel used. If a customer has PV output that most often looks like the data from a "bad" day, then they might choose to use a smaller flywheel and thus reduce the energy lost due to smoothing.

To analyze the cost, the motors need to be sized to handle the current applied through it, and for the load associated with it. For this simulation, two 5 kW motors (about \$800.00 each) were chosen to meet the energy production with a 6 kg flywheel was selected (costing of about \$200.00) for smoothing. With safety housing and sensor systems, the total cost of the system is estimated to cost about \$2,500.00. Cost of annual maintenance must also be considered. Additionally, cost for larger systems will also increase overall cost. As noted earlier in this discussion, the utility

provider is the beneficiary of this system, not the customer. For a customer, they would actually bear the burden of the losses, due to the inefficiency of the flywheel smoothing system. Unless the rate structure put some penalty cost on variance of the energy delivered to the grid, without other incentives by the utility, the consumer would not be motivated to install such a system. In order for the utility to implement this design, they would need to incentivize customers with benefits for installing this smoothing system.

4.1 Future Work

While this version of smoothing PV systems is effective, there are possibilities for use of an AC motor for the generation portion; however, more control is required to ensure the output frequency is consistent. The additional controls and components may cause efficiency loss, but may prove to be worthwhile in future applications. Future work includes evaluation of smoothing after the inverter, employing a AC motor and generator in series between the inverter and the grid connection. This system would require more complex controls to maintain necessary voltage magnitude, frequency and phase. Evaluation of this would require development of the mathematical and physical models, and the MATLAB simulation. Batteries in series with the PV array and ahead of the inverter may be a more attractive alternative than the use of motors and generators.

Batteries in parallel with the inverter, where energy can either go to the inverter or to charge the batteries, may have other advantages. One key question is: how much of the energy in high frequency components of the PV output can be usefully directed to charging of batteries (vs. being dissipated in the motor-flywheel-generator system studied in this thesis)? With batteries, particularly with them in series with the inverter, the DC supplied by the batteries to the inverter may be smoother and thus the output of the inverter may have less variation.

A hybrid system, batteries in conjunction with the flywheel smoothing, is another

possibility. Analysis for the parallel case, where the inverter uses the battery as a back-up supply, and the for the series case, either using the battery to filter the PV before the flywheel smoothing, or after, may result in better smoothing.

5 Conclusion

In this work we have demonstrated, via simulation and analysis, that a flywheel smoothing system, in series with a PV array and ahead of the inverter, can reduce the variations in energy used (or delivered) as seen by the distribution grid, for consumers with local renewable generation.

The simulation of this system in MATLAB SimPowerSystems was a significant component of this work. Several limitations of these tools were overcome to produce credible simulations. However, the benefits of this toolbox exceed that of other available options that could be used to simulate the smoothing effects of a flywheel.

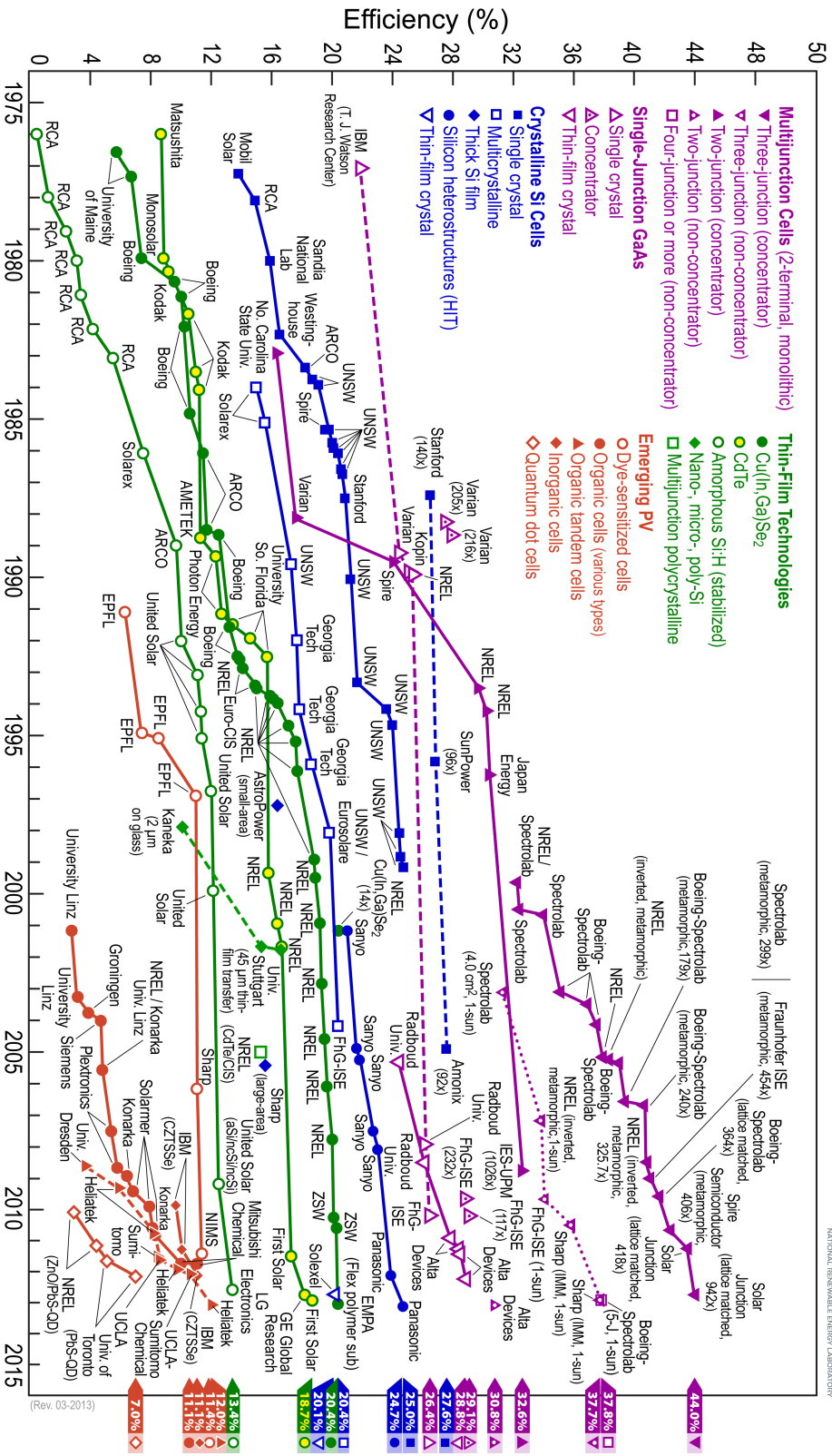
The external data used in the simulations was not ideal, since there exist no available data with a sampling frequency high enough to capture the high frequency variations from a PV array, or another renewable generation source.

The flywheel smoothing system does not benefit the consumer, on whose premises it needs to be installed, in any way. It is expensive, requires a large amount of space, requires maintenance, may be a noise source (not analyzed in this thesis), and it has some (minor) safety issues. While some incentive plan could be created by utilities to make installation of a flywheel smoothing system by consumers, this seems very unlikely under present conditions.

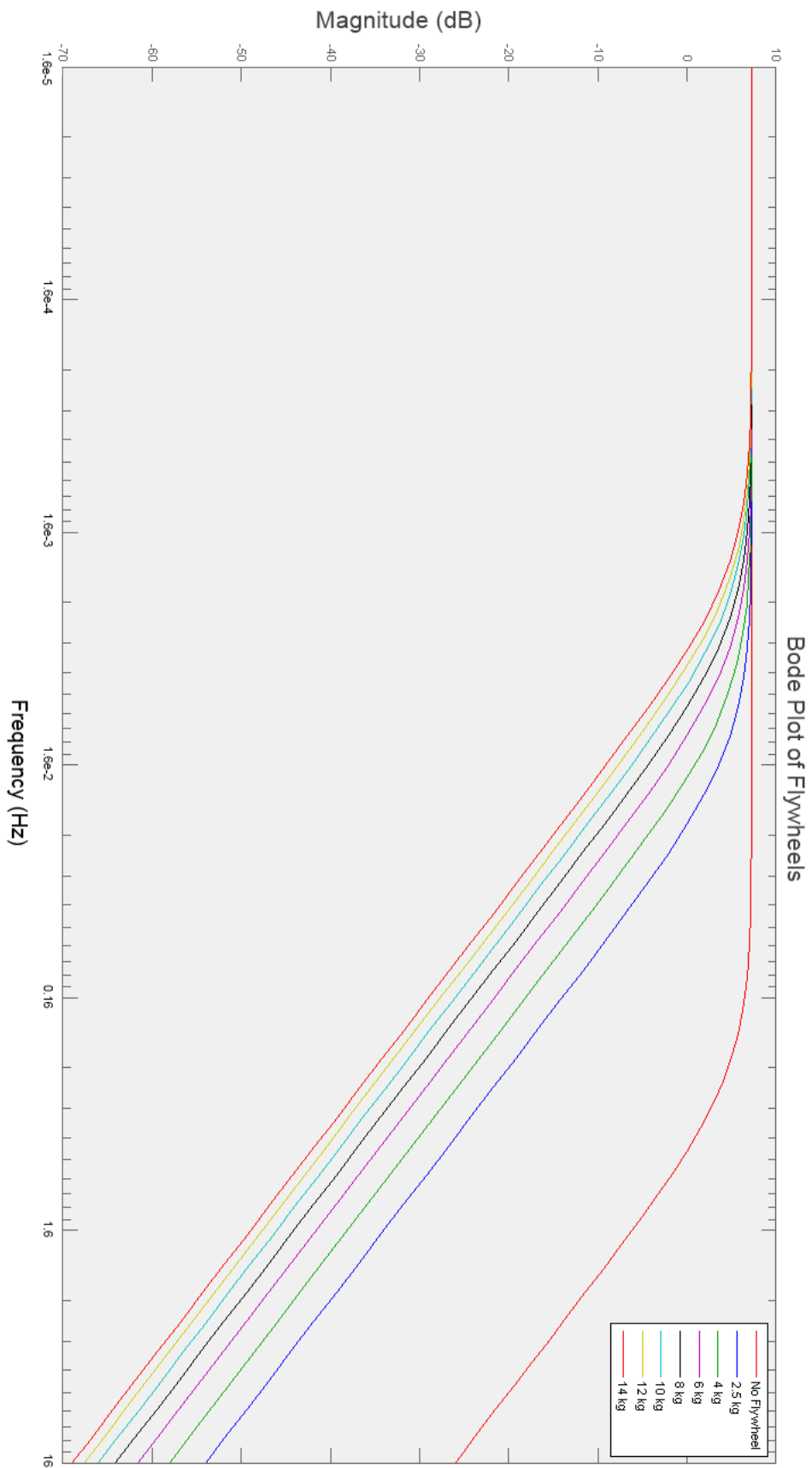
From all the parameters associated with the system, the functionality of the system does what is needed for utilities. The flywheel system smooths the power effectively and provides a wide variety of smoothing abilities for customer use. However, due to the added cost to an already pricey market, this system does not provide enough

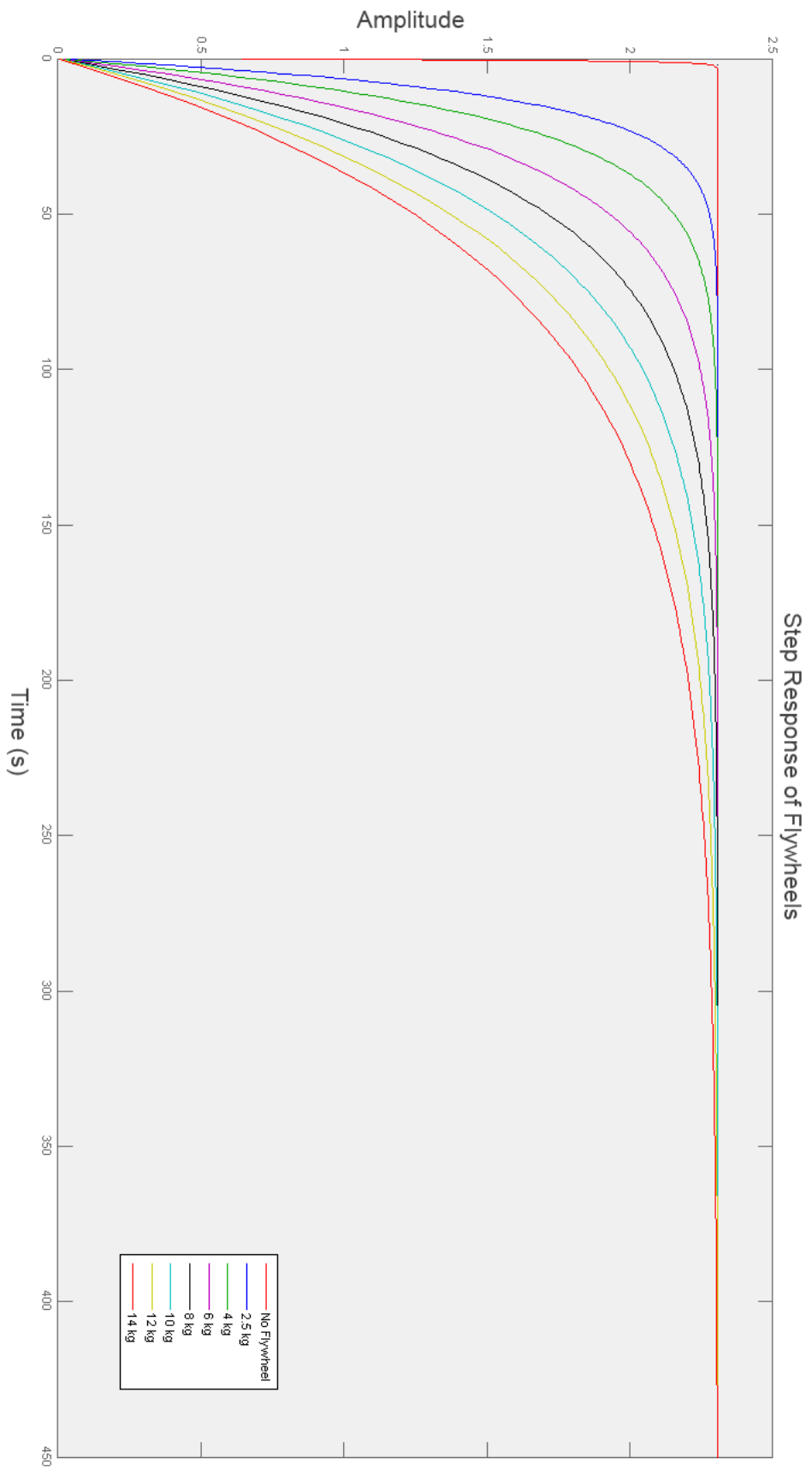
benefits for the customer to be feasible. Additionally, the flywheel wastes too much energy (around 20%) coming from the PV array due to smoothing. Until a proper rate structure can be developed, larger benefits to the customer can be proposed, or higher efficiency within the smoothing, the flywheel will remain impractical for existing and future renewable deployments. Further work on more intelligent use of batteries to absorb the PV output, including the higher frequency components, seems to be a more promising approach to smoothing of the effects on the distribution grid of renewable generation.

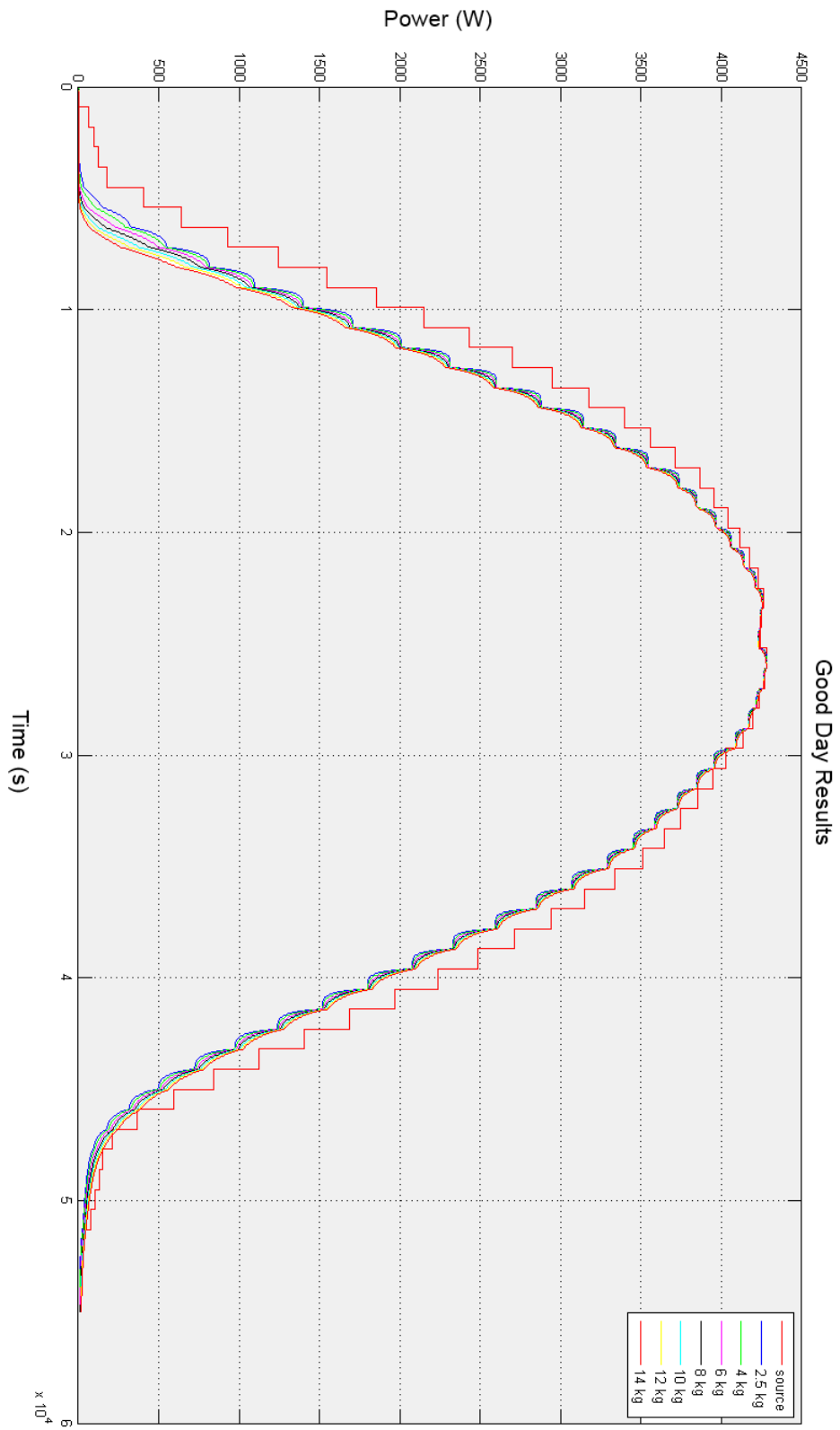
Best Research-Cell Efficiencies

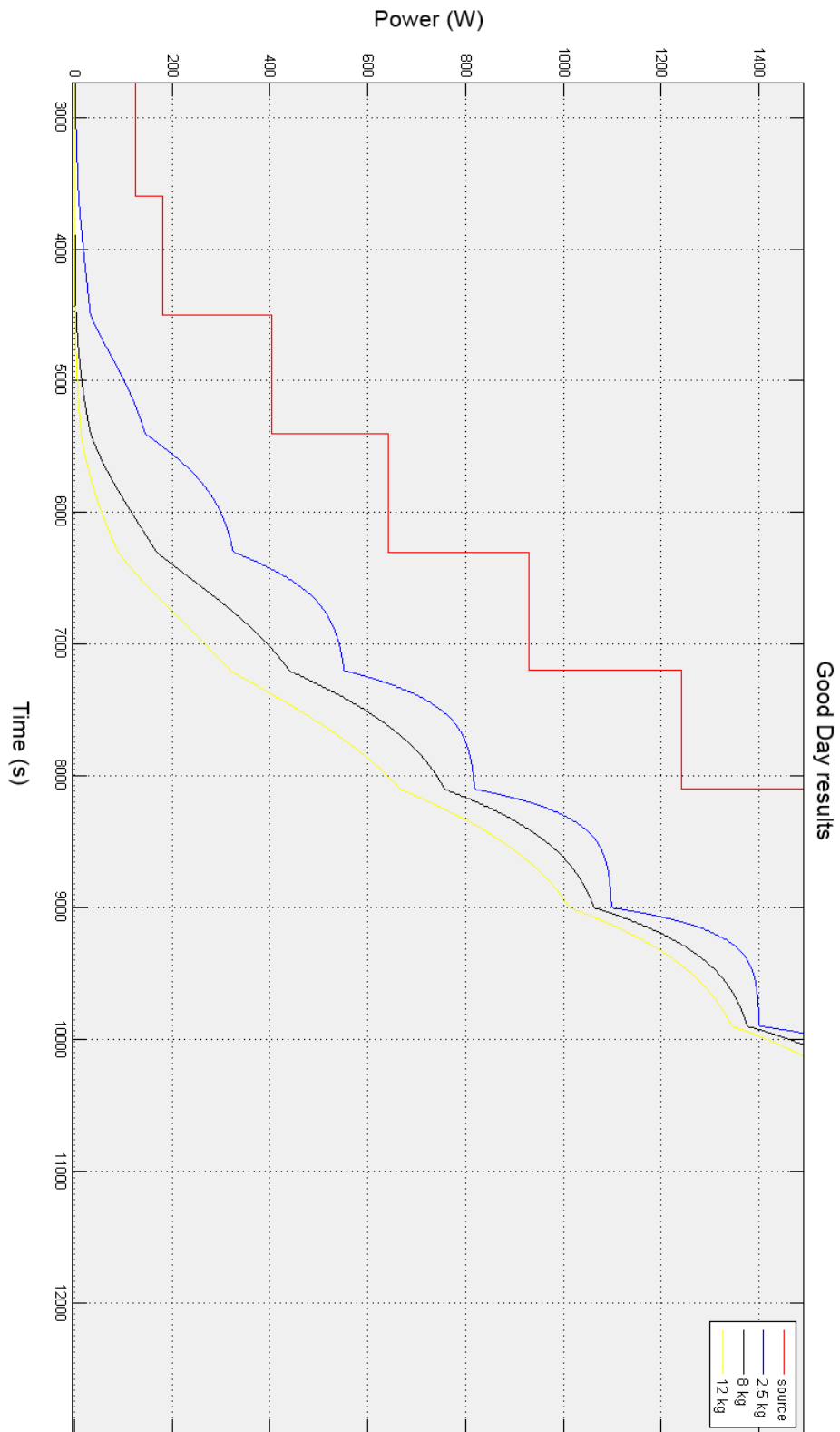


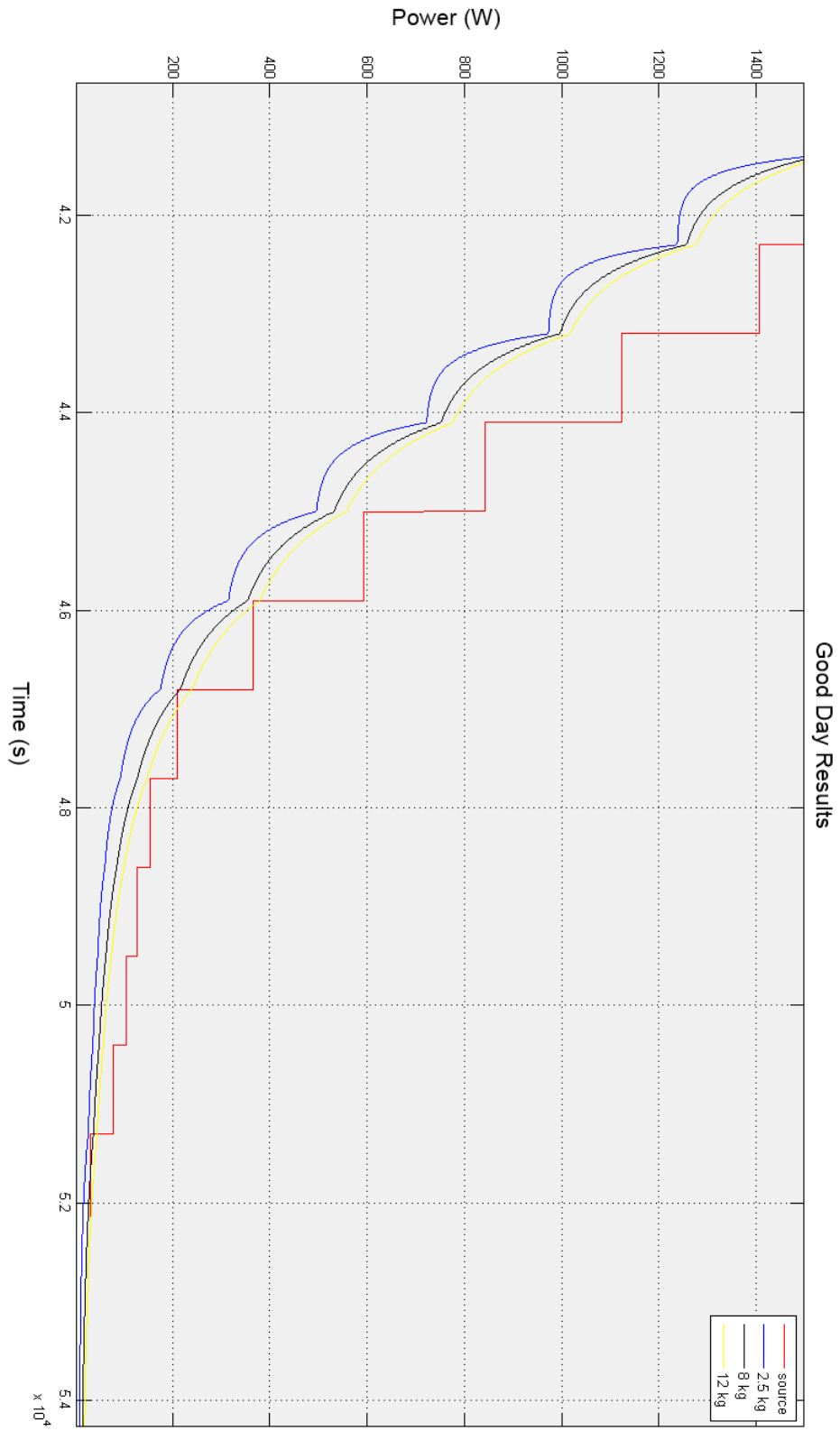
(Rev. 03-2013)



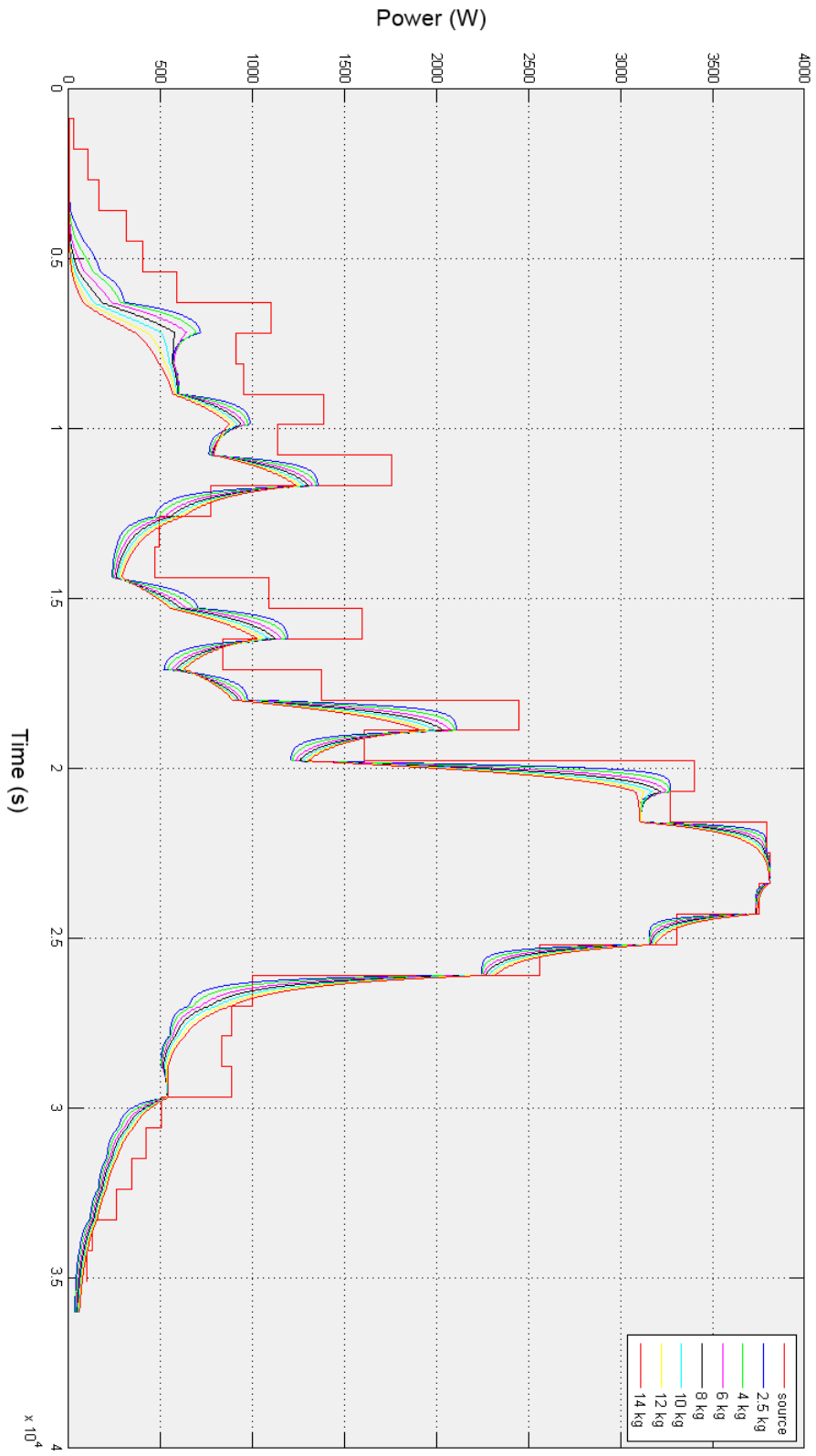


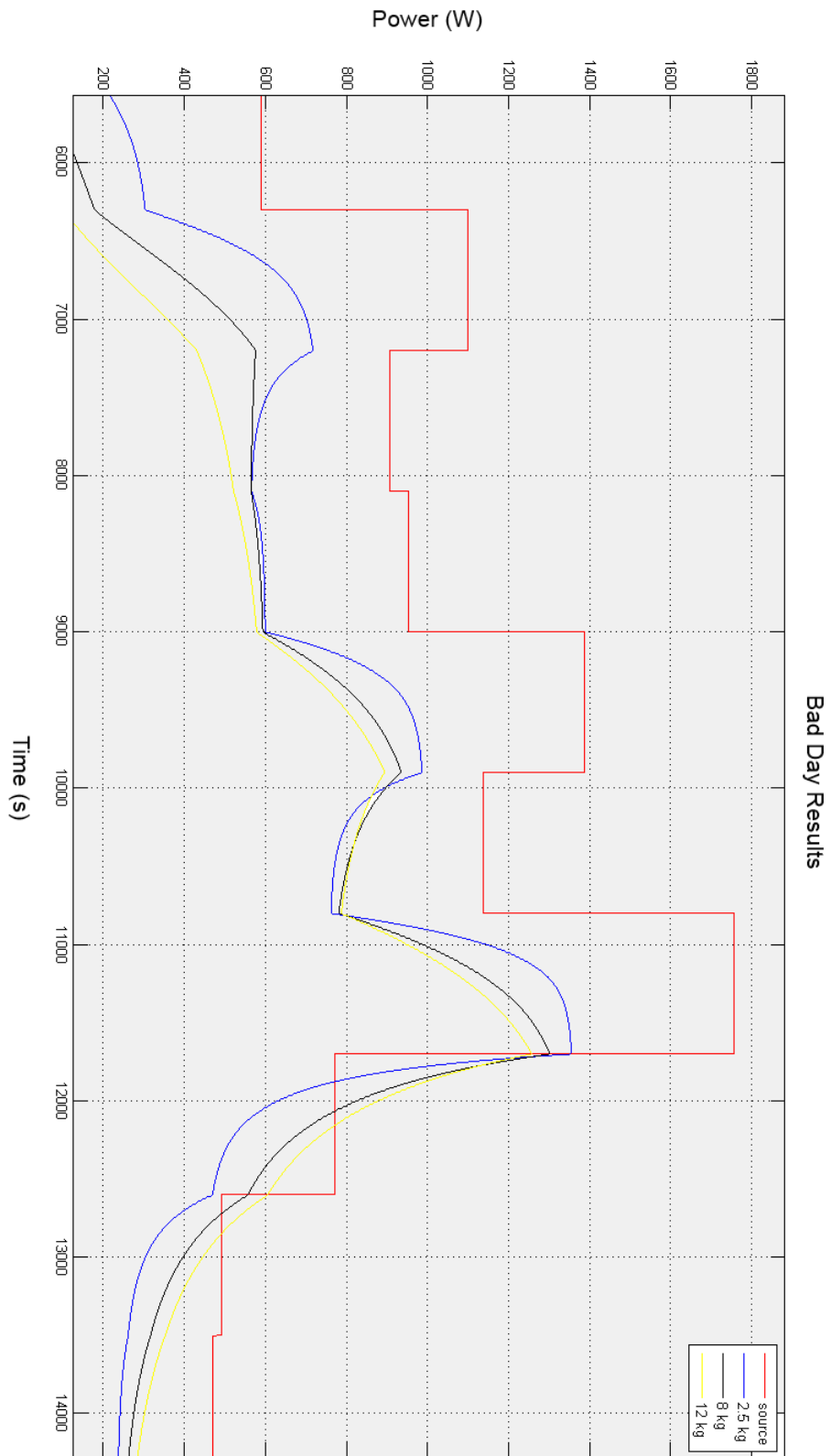






Bad Day Results





References

- [1] R. Arghandeh, M. Pipattanasomporn, and S. Rahman. Flywheel energy storage systems for ride-through applications in a facility microgrid. *Smart Grid, IEEE Transactions on*, 3(4):1955–1962, 2012.
- [2] R.S. Bhatia, S.P. Jain, D.K. Jain, and Bhim Singh. Battery energy storage system for power conditioning of renewable energy sources. In *Power Electronics and Drives Systems, 2005. PEDS 2005. International Conference on*, volume 1, pages 501–506, 2005.
- [3] R. Carbone. Grid-connected photovoltaic systems with energy storage. In *Clean Electrical Power, 2009 International Conference on*, pages 760–767, 2009.
- [4] Gauthier Delille and Bruno François. A review of some technical and economic features of energy storage technologies for distribution system integration. *Ecological engineering and environment protection*, (1):40–49, 2008.
- [5] Jinxu Ding and A. Somani. A long-term investment planning model for mixed energy infrastructure integrated with renewable energy. In *Green Technologies Conference, 2010 IEEE*, pages 1–10, 2010.
- [6] Karina Garbesi, Vagelis Vossos, and Hongxia Shen. Catalog of dc appliances and power systems. (LBNL-5364E), October 2011.
- [7] Pacific Gas and Electric. Voltage tolerance boundary.
- [8] M.E. Glavin, P.K.W. Chan, S. Armstrong, and W.G. Hurley. A stand-alone photovoltaic supercapacitor battery hybrid energy storage system. In *Power Electronics and Motion Control Conference, 2008. EPE-PEMC 2008. 13th*, pages 1688–1695, 2008.
- [9] Eiichi Haginomori. Emtp simulation of transient stability enhancement phenomena by an inverter controlled flywheel generator. *Electrical Engineering in Japan*, 124(3):19–29, 1998.

- [10] Thomas J. Overbye J. Duncan Glover, Mulukutla S. Sarma. *Power Systems: Analysis and Design*.
- [11] H. Kanchev, Di Lu, F. Colas, V. Lazarov, and B. Francois. Energy management and operational planning of a microgrid with a pv-based active generator for smart grid applications. *Industrial Electronics, IEEE Transactions on*, 58(10):4583–4592, 2011.
- [12] Jinho Kim and Jong-Hwan Lee. A model of stability. *Power and Energy Magazine, IEEE*, 9(1):75–81, 2011.
- [13] M. Liserre, T. Sauter, and J.Y. Hung. Future energy systems: Integrating renewable energy sources into the smart power grid through industrial electronics. *Industrial Electronics Magazine, IEEE*, 4(1):18–37, 2010.
- [14] J. McDowall. Conventional battery technologies-present and future. In *Power Engineering Society Summer Meeting, 2000. IEEE*, volume 3, pages 1538–1540 vol. 3, 2000.
- [15] NREL. Best research: Photovoltaic cell efficiencies. Technical report.
- [16] Sanyo / Panasonic. Hit photovoltaic module. Datasheet, 2012.
- [17] Sun-Jae Park, Joung-Hu Park, and Hee-Jong Jeon. Controller design of grid-connected power conditioning system with energy storage device. In *Electrical Machines and Systems (ICEMS), 2011 International Conference on*, pages 1–6, 2011.
- [18] K. Porter and the Intermittency Analysis Project Team. Intermittency analysis project: Summary of final results. california energy commission, pier research development & demonstration program. Technical report, CEC-500-2007-081.
- [19] P.F. Ribeiro, B.K. Johnson, M.L. Crow, A. Arsoy, and Y. Liu. Energy storage systems for advanced power applications. *Proceedings of the IEEE*, 89(12):1744–1756, 2001.

- [20] S. Samineni, B.K. Johnson, H.L. Hess, and J.D. Law. Modeling and analysis of a flywheel energy storage system for voltage sag correction. In *Electric Machines and Drives Conference, 2003. IEMDC'03. IEEE International*, volume 3, pages 1813–1818 vol.3, 2003.
- [21] Satish Samineni, Brian K Johnson, Herbert L Hess, and Joseph D Law. Modeling and analysis of a flywheel energy storage system with a power converter interface. In *International Conference on Power Systems Transients-IPST*, 2003.
- [22] T.A. Short. *Electric Power Distribution Equipment and Systems*. Taylor & Francis, 2006.
- [23] R. Thompson. Flywheel safety.
- [24] M.G. Villalva, T.G. de Siqueira, and E. Ruppert. Voltage regulation of photovoltaic arrays: small-signal analysis and control design. *Power Electronics, IET*, 3(6):869–880, 2010.
- [25] M.G. Villalva, J.R. Gazoli, and E.R. Filho. Comprehensive approach to modeling and simulation of photovoltaic arrays. *Power Electronics, IEEE Transactions on*, 24(5):1198–1208, 2009.
- [26] M.G. Villalva, J.R. Gazoli, and E.R. Filho. Modeling and circuit-based simulation of photovoltaic arrays. In *Power Electronics Conference, 2009. COBEP '09. Brazilian*, pages 1244–1254, 2009.
- [27] Ma Yiwei, Yang Ping, and Guo Hongxia. Development of distributed generation system based on various renewable energy resources. In *Control Conference (CCC), 2011 30th Chinese*, pages 6203–6207, 2011.
- [28] Long Zhou and Zhiping Qi. Modeling and simulation of flywheel energy storage system with ipmsm for voltage sags in distributed power network. In *Mechanics and Automation, 2009. ICMA 2009. International Conference on*, pages 5046–5051, 2009.